

REGIONALIZATION AND VARIABILITY OF PRECIPITATION IN HAWAII

Korine N. Kolivras

**Virginia Polytechnic Institute and State University
Department of Geography
115 Major Williams Hall
Blacksburg, Virginia 24061**

Andrew C. Comrie

**The University of Arizona
Department of Geography and Regional Development
Harvill Building, Box #2
Tucson, Arizona 85721**

Abstract: Regions based on seasonal precipitation variability for Hawaii are determined using a principal components analysis applied to 124 stations for the period 1971–2000. Nine regions are delineated and are consistent with known precipitation patterns; leeward and windward stations are in separate regions on all islands. Within each region, the relationship between precipitation and the El Niño–Southern Oscillation (ENSO) is examined using a correlation analysis with the Southern Oscillation Index (SOI), and the Niño 3.4 and Niño 1+2 indices. Precipitation is most frequently correlated with ENSO in the different regions using SOI and Niño 3.4. Using several nonparametric statistical tests, it is determined that while average precipitation received in Hawaii during El Niño events is significantly different from average precipitation (1971–2000) and from precipitation received during La Niña events, the relationship between precipitation and individual ENSO events within regions is rarely significant. Finally, during El Niño or La Niña events, average precipitation receipt across the regions co-varies during winter and summer under concurrent conditions and a one-season lag. Synoptic patterns are examined and indicate a deviation from average conditions during ENSO events that affects subsidence and precipitation patterns. [Key words: Hawaii, precipitation, regionalization, principal components analysis, El Niño–Southern Oscillation.]

INTRODUCTION

Numerous studies over the past several decades have identified the effects of the El Niño–Southern Oscillation (ENSO) on local climate conditions around the world. The shift in wind and pressure patterns along the equator, resulting in changes in sea surface temperatures, can lead to variability in precipitation and temperature patterns. ENSO, while a global phenomenon, has been linked to local impacts such as wildfires (Swetnam and Betancourt, 1992), flooding and droughts (Dilley and Heyman, 1995), and disease outbreaks (Hales et al., 1999; Kovats, 2000). It is with the latter local application that we are most interested; in particular, there may be an increased risk of mosquito-borne disease during El Niño or La Niña events in Hawaii, and therefore an evaluation of the effect of ENSO events at a sub-island scale is important. We are particularly interested in the seasonal timing of

precipitation and the effect of ENSO on precipitation across the islands because of the consequences for mosquito-borne disease such as the recent outbreak of dengue fever (Kolivras, 2006). Further, inter- and intra-island variability in precipitation can have important consequences for agriculture, tourism, and the understanding of island ecology and biogeography.

Hawaii is located within the tropics and, therefore, experiences a generally warm and moderate climate, but local climates of the islands are spatially varied, mainly because of topography. There is a high degree of variation in precipitation amount across the islands, and in addition, the seasonal timing of precipitation varies spatially as well, which is the focus of this study. The island chain has been referred to as a miniature continent, given that vegetation type ranges from desert scrub in dry locations, some of which receive less than 250 mm of rain annually, to tropical forests with Mt. Waialeale on Kauai receiving over 11,000 mm of rain annually (Sanderson, 1993). One source of precipitation variability in Hawaii is ENSO, and a number of studies have recognized a clear link between ENSO events and precipitation variability in Hawaii; the islands in general typically experience drought conditions following an El Niño event whereas above average precipitation is associated with La Niña events (Lyons, 1982; Chu, 1989; Sanderson, 1993; Chu and Chen, 2005). However, no published study to date has explicitly identified regions with common seasonal variability (rather than absolute precipitation amount) and connected this behavior to underlying ocean-atmosphere variations.

The objective of this research is to examine the relationship between ENSO and precipitation at the sub-island scale after regionalizing Hawaiian precipitation based on the seasonal pattern. Specifically, this study addresses the following research questions: (1) What regions related to the seasonal timing of precipitation can be clearly defined across the islands? (2) Which ENSO index is most strongly correlated with Hawaiian precipitation in each region? and (3) To what degree are all areas of the islands uniformly dry during El Niño and uniformly wet during La Niña?

BACKGROUND

Prior studies have examined particular aspects of Hawaii's climate across the islands as a whole (Lyons, 1982; Chu, 1989; Chu and He, 1994), while other studies have investigated climatic characteristics on particular islands or in vertical transects on islands (Riehl, 1949; Nullet and Giambelluca, 1992; Juvik and Nullet, 1994; Nullet et al., 1995; Ramage and Schroeder, 1999). Another set of studies has been devoted to exploring specific causes of climate variability, including ENSO. Patterns that may be associated with an El Niño-induced drought in Hawaii include a decreased number of synoptic storm systems reaching the islands and reduced trade wind rainfall associated with the shift of pressure centers (Lyons, 1982; Chu et al., 1993; Sanderson, 1993). Taylor (1984) found that the relationship between the Southern Oscillation and Hawaiian rainfall varies temporally during winter, and the use of canonical correlation analysis in predicting Hawaiian rainfall has shown that lagged sea level pressure and the Southern Oscillation Index (SOI) best predict winter precipitation (Chu and He, 1994). Barnston and He (1996) expanded upon this

study through the addition of sea surface temperature (SST) as a predictor variable and found that SST is also an important predictor of Hawaiian precipitation.

As with the impact of ENSO in other parts of the world, not every El Niño event results in a drought in Hawaii and not every drought is associated with El Niño (Lyons, 1982). Chu et al. (1993) contrasted the drought of 1980–1981 with the relatively wet year of 1982, both of which occurred in the absence of El Niño or La Niña, and hypothesized that changes in the Pacific/North American (PNA) teleconnection may have played a role. Additionally, the Pacific Decadal Oscillation (PDO) interacts with ENSO and results in varied precipitation; rainfall in Hawaii is negatively correlated with PDO (Chu and Chen, 2005). It has also been recognized that El Niño influences the number and path of tropical cyclones in the central Pacific (Chu and Wang, 1997; Chu and Clark, 1999; Clark and Chu, 2002).

While prior studies have confirmed the presence of a relationship between ENSO and island-wide precipitation variability in Hawaii, there is a need for an improved understanding of the relationship at a finer spatial detail. Complex spatial precipitation patterns are present across Hawaii because of the effect of island terrain interacting with the trade winds, the subsidence inversion, and tropical cyclones (Sanderson, 1993), and therefore for studies within the islands, a regionalization can provide a useful way to study the spatial and temporal variability in precipitation within the state. In this study, a principal components analysis (PCA) is used to identify seasonal precipitation regions with common temporal behavior across Hawaii. No studies have explicitly attempted to produce regions indicating the seasonal timing of precipitation in Hawaii, although others have examined spatial patterns of precipitation quantity using a regional context. Stidd and Leopold (1951) studied the high level of spatial variation in mean monthly rainfall across the islands, and attributed that variation to cyclonic and orographic rainfall patterns. Giambelluca et al. (1986) reported spatial variation in rainfall maxima and minima on each island, and in a separate study examined spatial patterns connected to drought at the sub-island level (Giambelluca et al., 1991). The study presented here contributes generally to the body of literature on sub-island precipitation patterns by evaluating the effects of ENSO on rainfall at a regional scale across the islands.

The same general technique (empirical orthogonal function analysis) as that used in this study (PCA) was used with a covariance matrix to divide areas of Hawaii according to dominant causes of rainfall quantity (Lyons, 1982). Our study uses a correlation matrix instead to examine the variability and seasonal timing of precipitation, rather than absolute amounts, as a way to identify common causes of precipitation variability in the islands. Additionally the Lyons study resulted in the delineation of three regions, and some applications, such as our follow-on study examining mosquito-borne disease, require more than three regions for examining precipitation variation. While Lyons (1982) evaluated El Niño and Hawaiian precipitation, the relationship was examined for the island chain as a whole using average precipitation at 63 stations. The goal here is to study the nature of sub-island variability and to determine if the effects of ENSO are uniform across the islands or not by incorporating data from a larger number of stations (124), which also provide more detail for the regionalization than the Lyons study.

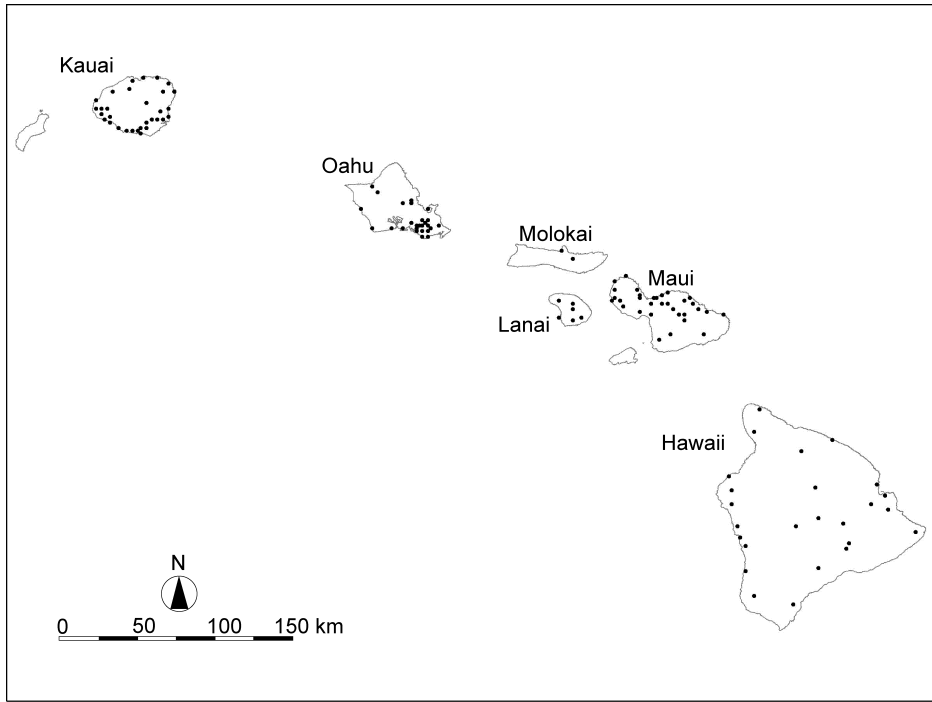


Fig. 1. Location of stations eligible for inclusion in the study. The 124 stations are spread fairly consistently across the largest islands (Kauai $n = 31$, Oahu $n = 28$, Molokai $n = 2$, Lanai $n = 6$, Maui $n = 32$, Hawaii $n = 25$), although spatial coverage on individual islands is not always even.

DATA

Monthly precipitation data for 1971 to 2000 were obtained for stations across Hawaii from the National Climatic Data Center (NCDC). This time period was selected rather than the period of record for each station in order to have a common time series for the PCA; while some stations have a longer period of record, requiring a longer time series would have excluded a considerable number of stations, which would have resulted in an insufficient representation of the overall spatial variability. Specifically, extending the period of record back ten to thirty additional years would have resulted in approximately a 50% reduction in the number of stations included in the PCA. While a somewhat arbitrary delimitation, stations could have no more than 4% missing data in order to be eligible for inclusion in the study, which equals approximately one year of data. Because of missing data, some stations that would have created a more even and representative spatial distribution were excluded so that stations remaining in the study had a relatively thorough data record to satisfy the needs of the PCA. Missing precipitation data were replaced with the monthly mean, and the resulting dataset included 124 stations (Fig. 1). Stations included in the study are broadly distributed across the four large islands, although as expected, there was a lower density of high elevation stations eligible for the study.

Three indices, Niño 1+2, Niño 3.4, and SOI, were selected to evaluate the relationship between precipitation and ENSO in this study and were acquired from the Climate Diagnostics Center (CDC; <http://www.cdc.noaa.gov>). Niño 1+2 and Niño 3.4 are temperature-based indices developed using mean sea surface temperatures in different areas of the equatorial Pacific Ocean (Hanley et al., 2003). The Niño 1+2 area is located just off the coast of South America, from the equator to 10°S, while the Niño 3.4 area straddles the equator (5°N to 5°S) from about 170°W to 120°W. SOI is calculated by the Climate Prediction Center as the difference in standardized atmospheric pressure between Tahiti and Darwin, Australia (Climate Prediction Center, 2005). Given that the Niño 3.4 index is developed from an area of the tropical Pacific Ocean that overlaps with the Niño 3 (eastern Pacific) and Niño 4 (western Pacific) indices, and is highly correlated with them, Niño 3.4 was chosen to represent the central equatorial Pacific.

METHODS

For the regionalization, a principal components analysis was applied to the monthly precipitation data using a correlation matrix to emphasize the relative amount and seasonal timing of precipitation, rather than total precipitation amount (Comrie and Glenn, 1998). Thus, areas with more or less absolute rainfall, but with the same relative variability, are considered to be influenced by the same processes causing the common variability. The components were rotated using the direct oblimin (oblique) rotation, which generally shows the most coherent and stable patterns in a climate regionalization while avoiding artifacts in the mapped patterns (White et al., 1991). Thirteen components were initially retained based on scree plots and eigenvalues > 1 , explaining 83.6% of the variance in the data. Following Comrie and Glenn (1998), the rotated loading values (γ) for each component were mapped by station and interpolated using the inverse distance weighting method. Regions were then created using the $\gamma = \pm 0.4$ contours as borders. In order to confirm the coherence of the regions and verify the boundaries created by the contour lines, each station was assigned to the component on which it loaded most highly, and those maximum loadings were plotted on the region map (Comrie and Glenn, 1998). Areas lacking representative station coverage were excluded from the regionalization and marked "insufficient data." An additional PCA using a subset of stations served to evaluate and verify the regionalization.

An examination of the relationship between seasonal precipitation and the three ENSO indices was conducted within each region using a correlation analysis with concurrent conditions, and a one-season and two-season lag. However, temporal autocorrelation is present in the ENSO indices, and therefore an effective sample size adjustment was attempted in order to account for the autocorrelation (Thiebaut and Zwiers, 1984). Additionally, the relationship between winter SOI and the Niño 3.4 index, and concurrent precipitation in each region was examined visually through the creation of scatterplots. Chu (1989) used similar scatterplots to compare spring SOI and winter precipitation for the islands as a whole, and an examination of the relationship at the sub-island level presented here builds on that research. For this study, an El Niño event is defined as $SOI < -0.5$ and $Niño\ 3.4 <$

Table 1. Moderate and Strong El Niño and La Niña Events Selected for Analysis

El Niño	La Niña
1972–1973	1973–1974
1982–1983	1975–1976
1986–1987	1988–1989
1987–1988	1998–1999
1991–1992	1999–2000
1994–1995	
1997–1998	

0.4, a La Niña event as $SOI > 0.5$ and $Niño\ 3.4 > 0.4$, and a neutral event as $-0.5 > SOI < 0.5$ and $-0.4 > Niño\ 3.4 < 0.4$.

Two six-month seasons were used in this study, based on seasonal precipitation plots created during the PCA. In this study, winter was defined as November through April and summer as May through October. Although others have used seven- and five-month seasons (Giambelluca et al., 1986), an uneven seasonal division would have made lagged comparisons more difficult to interpret and our seasonal divisions are appropriate given the seasonal distribution illustrated in the precipitation plots.

Moderate and strong El Niño and La Niña events (Table 1) were selected based on classification by the Climate Prediction Center (Climate Prediction Center, 2006). There are other years that are close to the threshold for El Niño and La Niña events, but we selected the Climate Prediction Center's standard for the purposes of this research. Average winter and summer precipitation in each region was calculated for both El Niño and La Niña years, which was then represented as a percentage of the 1971–2000 average. Several statistical tests were used to evaluate the inter-region precipitation differences during El Niño and La Niña, and differences in precipitation receipt between El Niño and La Niña across the islands. Given the small number of years (30) available for this analysis, nonparametric tests were appropriate for use (Sprent, 1993). Wilcoxon signed ranks tests were used to determine if average precipitation received during El Niño years was statistically different from precipitation received during La Niña years, and from the overall 1971–2000 average precipitation receipt for both winter and summer across all regions. The statistical relationship between El Niño and La Niña precipitation receipt was evaluated within each individual region using a Mann-Whitney U-test. Precipitation receipt within each region during individual El Niño events was compared to precipitation receipt during individual La Niña events, as well as average precipitation receipt.

Finally, Kruskal-Wallis tests, the nonparametric equivalent of ANOVA (Sprent, 1993), were performed to evaluate inter-region differences in deviation from average winter and summer precipitation separately for El Niño and La Niña events. The Kruskal-Wallis test determines if a difference exists among three or more groups of data, and further testing is required to determine which groups differ. In this study,

we examined differences in average winter precipitation during El Niño and La Niña among the regions.

Lastly, composite synoptic patterns were examined to better understand the atmospheric drivers of the variation in precipitation received during El Niño and La Niña. The synoptic climatological links between ENSO and precipitation were examined by comparing precipitation totals and atmospheric circulation patterns for the selected El Niño and La Niña years. Composite maps for average conditions and ENSO events were constructed using NCEP/NCAR Reanalysis data (Climate Diagnostics Center, 2005). Geopotential heights at 1000 mb, 850 mb, 700 mb, and 500 mb were examined as well as outgoing longwave radiation (OLR) and vector wind direction and speed during neutral, El Niño and La Niña conditions. Geopotential heights were examined at multiple levels due to the presence of the subsidence inversion over Hawaii (Sanderson, 1993).

RESULTS

Region Designation

An initial solution of 13 principal components was selected, and with boundaries drawn based on the ± 0.4 loading contour, most (but not all) of the 13 regions had a clear center and covered a unique portion of a particular island. Component 9 had no stations that loaded at or above ± 0.4 and the contours showed no clear pattern in which a specific region could be discerned; it was therefore removed from the analysis. Components 7 and 12, centered on northwestern Maui and Lanai, had very similar seasonal precipitation patterns that were strongly correlated with one another, and given that component 12 comprised only one station, the two components were collapsed into one region. Finally, the two stations that comprised component 11, located on Kauai and Maui, were instead allocated to components 6 and 3 respectively to create geographical contiguity. This decision was justified because the 30-year precipitation time series for each of the two stations was highly correlated with the average time series for the final region in which it was included.

The creation of a final region map identifying areas based on unique seasonal precipitation patterns was based on the results of the principal components analysis, guided by the contour loadings maps and maximum loading stations maps (Comrie and Glenn, 1998). Initial region boundaries were created following the $\gamma = \pm 0.4$ contour line boundaries as a practical but arbitrary delimitation. Stations without strong loadings on any single component were generally included in the region on which they loaded most highly or within the region to which the full 30-year time series for each station was most highly correlated. For example, the northern end of the Big Island was not represented in any region according to the $\gamma = \pm 0.4$ contour lines, but the full precipitation time series for stations in that area were most strongly correlated with the average time series for region 3 (lowland Maui). Final region boundaries (Fig. 2) approximately follow the $\gamma = \pm 0.4$ contour line boundaries but include some stations outside of these areas that are defined by the maximum loading rule. Given that our focus is on the seasonal timing of precipitation,

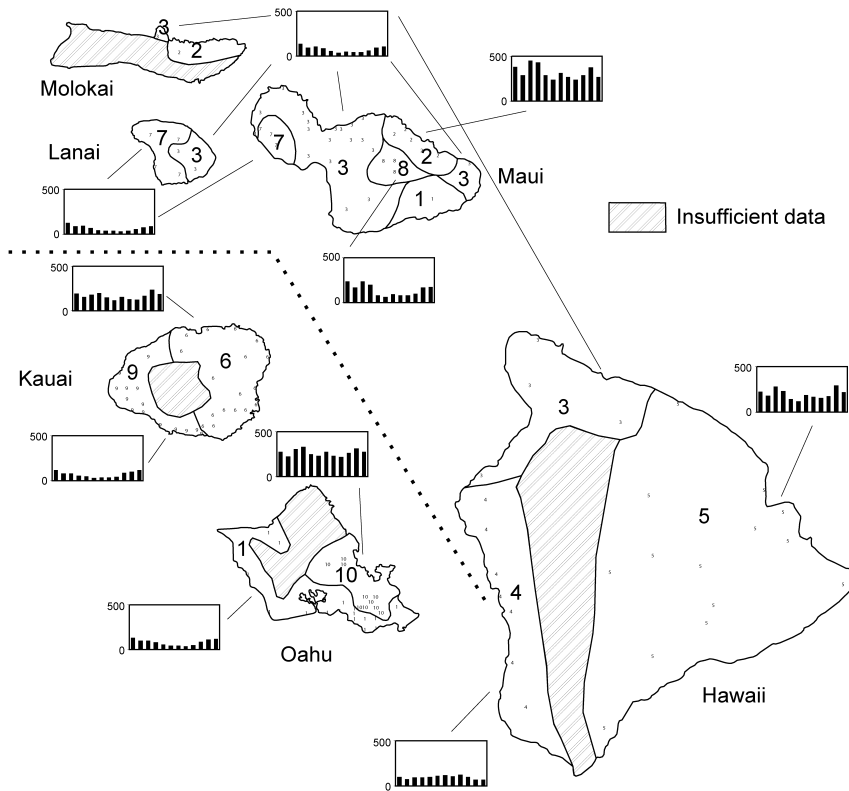


Fig. 2. Final region boundaries and the average annual precipitation graph for the stations in each region. Monthly precipitation totals range from 440 mm in region 2 to 1 mm in regions 7 and 9. Regions are defined based on the seasonal pattern of precipitation, rather than total precipitation.

regions include areas with a large range in rainfall quantity and a variety of terrain-related differences if the precipitation varied similarly on a seasonal basis. Additionally, locations both above and below the trade wind inversion, for example, might be affected similarly or differently by ENSO, and whether or not they should be considered separately or together (in the same region) based on the seasonality of precipitation is implicit in our approach.

To verify the results of the regionalization, a second PCA was conducted using a subset of the original data. One-third of the original stations were randomly excluded from the analysis, and the essential patterns found in the full analysis were supported. Regions delineated with the less spatially representative subset of the data were generally the same as those delineated using the full set of stations.

Region Characteristics

The annual precipitation graphs for each region (Fig. 2) illustrate the different seasonal cycles across the islands. Even though some average graphs appear

similar, the overall 30-year time series used vary enough that the areas were separated into different regions in the PCA. In the following discussion of the seasonal characteristics of each region, those regions with a relatively strong seasonal signal will be discussed first, followed by regions with a less obvious seasonal signal.

Low rainfall areas typically have a more obvious seasonal pattern than the windward locations that are commonly wet year-round (Giambelluca et al., 1986). Leeward Oahu (region 1), leeward Maui and Lanai (region 7), leeward Kauai (region 9), and lowland Maui/northern Hawaii (region 3) are generally dry on an annual basis since most are in a rainshadow location, and all receive the bulk of rainfall during the winter months when synoptic systems affect the state (Giambelluca et al., 1986). Subtle differences exist between leeward regions, with some locations receiving more rainfall than others during spring or fall. Leeward Hawaii (region 4) is unique among those regions with more apparent seasonal patterns in that the area experiences a summer peak in rainfall rather than a winter peak. During summer, the persistent trade winds frequently converge with onshore breezes, producing a summer precipitation maximum along the Kona coast on the western side of the island (Giambelluca et al., 1986). High-elevation Maui (region 8) has a strongly seasonal precipitation pattern. The three stations that form the region, with elevations ranging from 1300 m to 2100 m are near the bottom boundary of the inversion layer, the height of which can vary upslope and downslope (Giambelluca and Nullet, 1991; Nullet and Giambelluca, 1992). Summer is relatively dry in this area, but considerable rainfall is received during winter and early spring.

Monthly precipitation graphs for the four windward regions, region two (windward Maui), region five (windward Hawaii), region six (windward Kauai) and region ten (windward Oahu) depict the tri-modal precipitation pattern that often characterizes areas of high rainfall in Hawaii (Giambelluca et al., 1986). Orographic lifting of the tradewinds, which are more persistent during summer, results in high rainfall during that season, while any decrease in precipitation during winter due to a decrease in strength of the tradewinds is offset by rainfall received from synoptic systems (Giambelluca et al., 1986).

ENSO Relationships

Correlation analysis. Table 2 shows the results of the correlation analysis between the three ENSO indices used in this analysis and concurrent seasonal precipitation in each region identified by the PCA. Based on an examination of autocorrelation in the data and the effective sample size adjustment, temporal autocorrelation among the ENSO indices was very high, and therefore the relationship between precipitation and ENSO could not be examined using time lags as initially proposed.

Some regions have very similar patterns of significant correlations, while others are quite different. Leeward Oahu (region 1) and leeward Hawaii (region 4) have identical patterns, and precipitation in those regions is correlated with all three indices during winter only. In both regions, Niño 1+2 and SOI indicate that El Niño (La Niña) is related to below (above) average precipitation during concurrent conditions. The Niño 3.4 analyses indicate a more complicated relationship between

Table 2. Statistically Significant ($\alpha = .05$) Pearson's Product-Moment Correlation Coefficients between Summer and Winter Precipitation and Three ENSO Indices under Concurrent Conditions^a

	Summer PPT	Winter PPT
Region 1 leeward Oahu		
Niño 1+2		<i>-.4306</i>
Niño 3.4		<i>.4919</i>
SOI		<i>.5018</i>
Region 2 windward Maui		
Niño 1+2	<i>.3741</i>	
Niño 3.4	<i>.4290</i>	
SOI	<i>-.3611</i>	
Region 3 lowland Maui		
Niño 1+2		
Niño 3.4	<i>.4451</i>	<i>.4214</i>
SOI	<i>-.4048</i>	
Region 4 leeward Hawaii		
Niño 1+2		<i>-.4211</i>
Niño 3.4		<i>.4370</i>
SOI		<i>.4862</i>
Region 5 windward Hawaii		
Niño 1+2		<i>-.4902</i>
Niño 3.4	<i>.5484</i>	
SOI	<i>-.5158</i>	<i>.5762</i>
Region 6 windward Kauai		
Niño 1+2		<i>-.3833</i>
Niño 3.4	<i>.3756</i>	<i>.3877</i>
SOI		<i>.4789</i>
Region 7 leeward Maui/Lanai		
Niño 1+2	<i>.4253</i>	
Niño 3.4	<i>.5790</i>	<i>.4998</i>
SOI	<i>-.4847</i>	
Region 8 highland Maui		
Niño 1+2		
Niño 3.4	<i>.4346</i>	<i>.4008</i>
SOI	<i>-.3647</i>	
Region 9 leeward Kauai		
Niño 1+2		<i>-.3791</i>
Niño 3.4	<i>.5120</i>	<i>.4217</i>
SOI	<i>-.5504</i>	<i>.4638</i>
Region 10 windward Oahu		
Niño 1+2		<i>-.4161</i>
Niño 3.4		
SOI		<i>.5116</i>

^aItalicized correlations significant at $\alpha = .01$.

sea surface temperature and precipitation in regions 1 and 4. Niño 3.4 is positively correlated with winter precipitation under concurrent conditions, meaning that warm sea surface temperatures (El Niño) are associated with above average rainfall. Lowland Maui (region 3) and highland Maui (region 8) have the same correlation patterns. Niño 1+2 is not significantly correlated with precipitation in either region. Niño 3.4 is positively correlated with concurrent summer and winter rainfall in both regions. Finally, SOI is correlated with concurrent summer precipitation in both regions.

Precipitation on leeward Maui/Lanai (region 7) and leeward Kauai (region 9) is significantly correlated with the ENSO indices under concurrent conditions. Niño 3.4 is positively correlated with both concurrent summer and winter precipitation in both regions. SOI is negatively correlated with concurrent summer precipitation in both regions but is positively correlated with winter precipitation only in region 9, leeward Kauai.

The four windward regions, for the most part, have unique patterns of correlation. Windward Maui/Molokai (region 2) has the most consistent pattern in that summer precipitation is correlated with all three indices at concurrent conditions with El Niño (La Niña) corresponding with above (below) average precipitation. Winter precipitation in region 2 is not significantly correlated with any index. Windward Hawaii (region 5) and windward Kauai (region 6) have somewhat similar correlation patterns, with winter precipitation negatively correlated with Niño 1+2. Summer precipitation in both regions 5 and 6 is positively correlated with concurrent Niño 3.4, and region 6 adds a significantly positive correlation with concurrent Niño 3.4 and winter precipitation. Finally, SOI is positively correlated with winter precipitation in both regions. Given these patterns, in regions 5 and 6 it appears that El Niño is related to below average winter precipitation and above average summer precipitation. Of all the regions, windward Oahu (region 10) has the fewest number of significant correlations, and those correlations that are significant involve winter precipitation. SOI is positively correlated with precipitation and Niño 1+2 is negatively correlated with concurrent winter precipitation. Therefore, El Niño (La Niña) conditions result in below (above) average winter precipitation in region 10.

Summarizing the overall relationships between precipitation and the ENSO indices, some interesting patterns are revealed. Niño 1+2 is always negatively correlated with winter precipitation in regions with a significant relationship; summer precipitation is significantly positively correlated with Niño 1+2 in only a few cases. Therefore, according to the relationship between Niño 1+2 and precipitation, El Niño (La Niña) conditions result in below (above) average winter precipitation and above (below) average summer precipitation. Niño 3.4 is always positively correlated with both summer and winter precipitation if there is a significant relationship. In regions that had a significant relationship between SOI and precipitation, the correlation in summer is positive and the correlation in winter is negative in every case. Therefore, using SOI, whether in a leeward or windward location, El Niño is associated with above average rainfall in summer and below average rainfall in winter, and the opposite pattern is evident for La Niña.

Scatterplots for concurrent winter conditions reveal the variability in precipitation receipt according to SOI (Fig. 3) and Niño 3.4 (Fig. 4). In all regions, highly

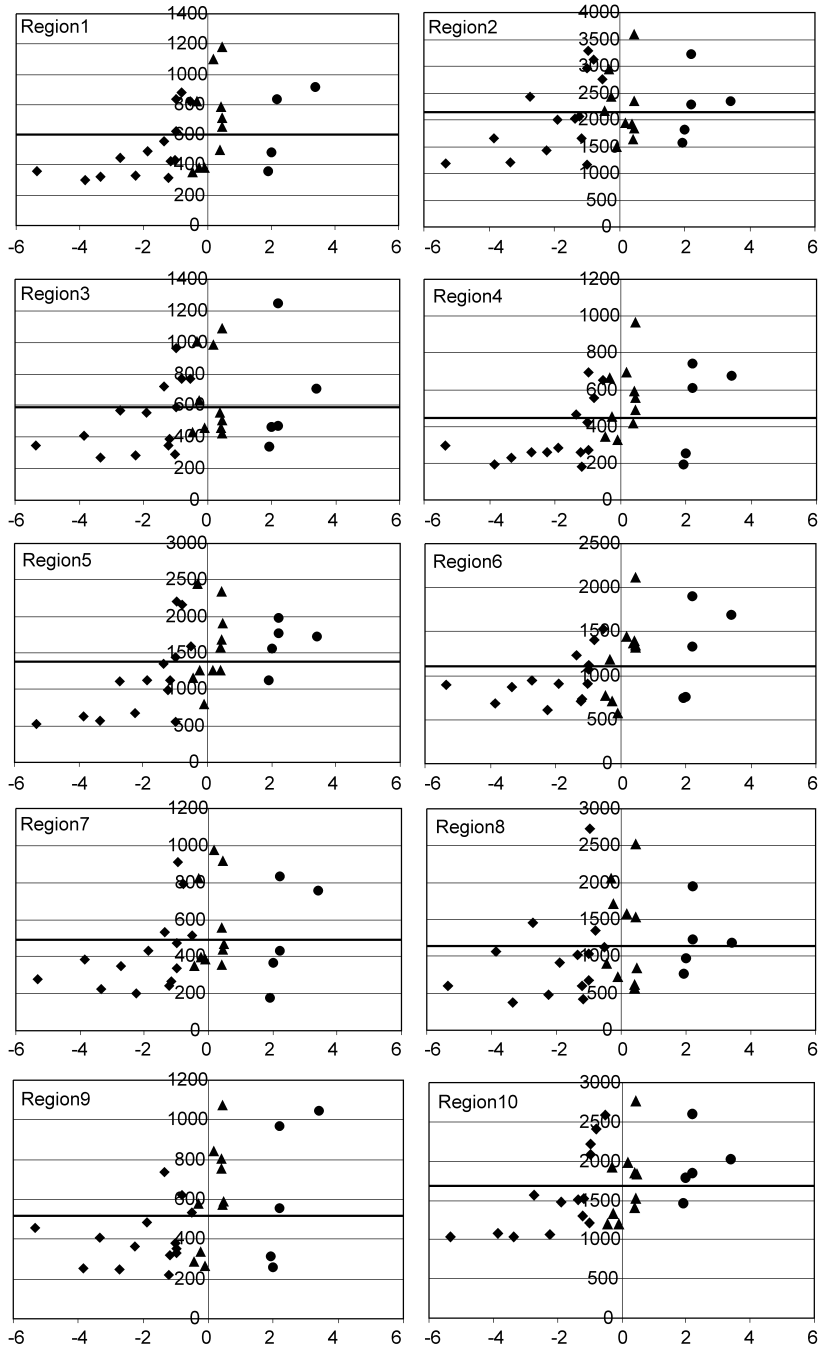


Fig. 3. Scatterplots comparing SOI (x-axis) and precipitation (y-axis) in each region show the variability in winter precipitation receipt (mm) by phase of ENSO. El Niño events (diamonds) are typically dry, while neutral (triangles) and La Niña events (circles) can range from wet to dry. Statistically significant ($\alpha = .05$) correlations are found in regions 1, 4, 5, 6, 9, and 10.

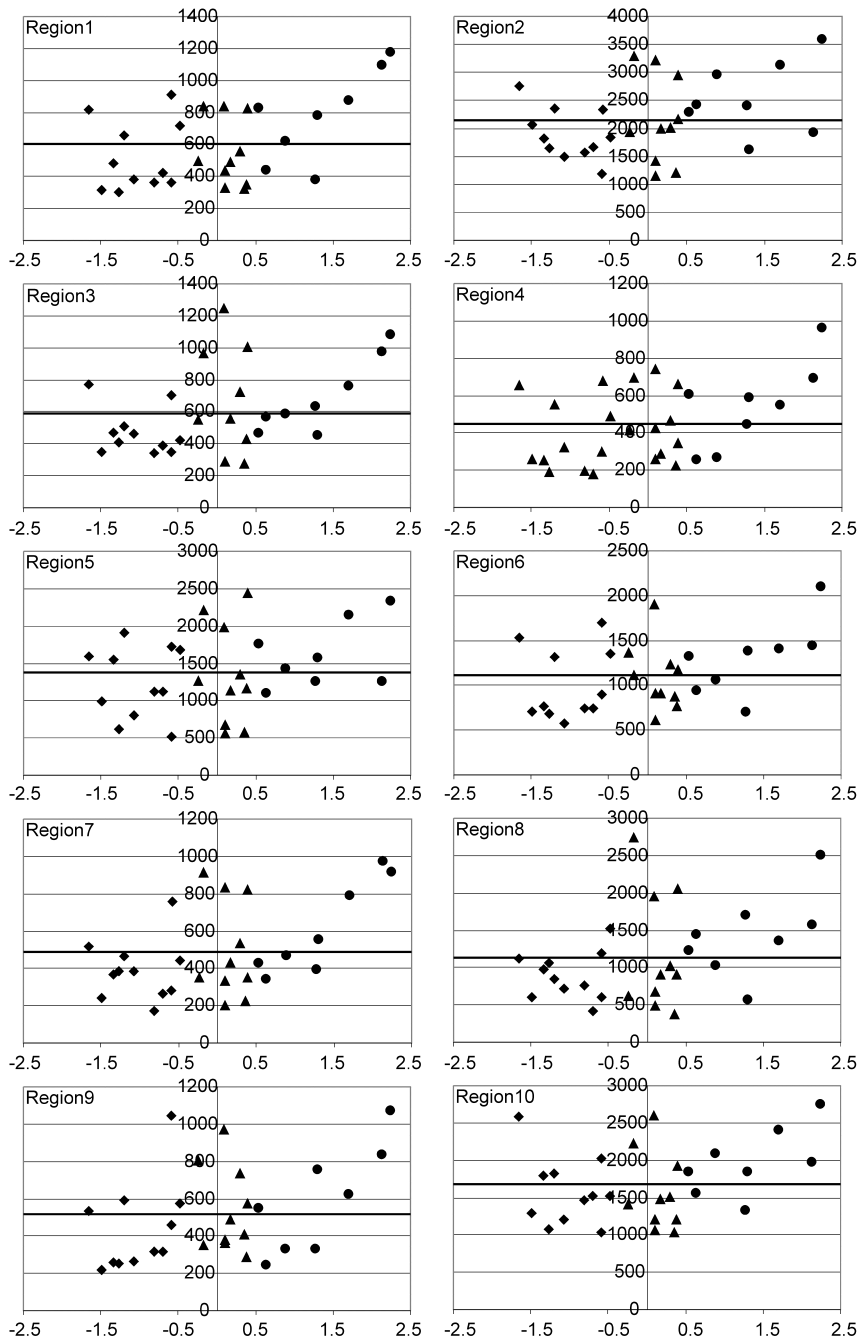


Fig. 4. Scatterplots comparing Niño 3.4 values (x-axis) and precipitation (y-axis) in each region show the variability in winter precipitation receipt (mm) by phase of ENSO. The relationship between Niño 3.4 and precipitation is generally not as clear as the relationship between SOI and precipitation (Fig. 3). Statistically significant ($\alpha = .05$) correlations are found in regions 1, 3, 4, 6, 7, 8, and 9. El Niño events = diamonds, neutral = triangles, and La Niña events = circles.

Table 3. Average Precipitation Receipt during El Niño Versus La Niña, Based on Wilcoxon Signed Ranks Test^a

Winter precipitation	<i>p</i> -value	Summer precipitation	<i>p</i> -value
La Niña and El Niño	<i>.005</i>	La Niña and El Niño	.445
La Niña and average	<i>.005</i>	La Niña and average	<i>.013</i>
El Niño and average	<i>.005</i>	El Niño and average	.508

^aSignificant *p*-values italicized.

negative SOI (El Niño) corresponds with precipitation that is below average while neutral and positive SOI range from below average to above average precipitation. While not all El Niño events result in below average rainfall, the relationship is more consistent than that of La Niña or neutral events; precipitation variability in all regions is greater during neutral and La Niña events. Therefore, for prediction purposes based on SOI, El Niño is likely to result in below average precipitation but La Niña or neutral events may result in below or above average precipitation across all regions. Niño 3.4 scatterplots show a similar relationship between the index and precipitation, but it is less clear than that of SOI and precipitation. Generally, El Niño, as defined by Niño 3.4, results in below average precipitation and La Niña results in above average precipitation, but there is considerable variation from event to event.

Comparison of El Niño and La Niña Years

The Wilcoxon signed ranks tests indicate that overall winter precipitation receipt during El Niño events is significantly different ($\alpha = .05$) from precipitation receipt during La Niña events, and from average precipitation, during the concurrent winter (Table 3). Additionally, winter precipitation during La Niña is significantly different from average as well. During the following summer, precipitation during La Niña events is significantly different from average, but there is not a significant relationship between precipitation received during El Niño and La Niña, nor El Niño precipitation receipt and average. Overall, there is a significant relationship between both El Niño and La Niña and concurrent winter precipitation, but for summer, there is only a significant relationship between La Niña and summer precipitation.

When the relationship between ENSO events and precipitation is examined within each region using a Mann-Whitney U-test, few statistically significant relationships are found (Table 4). Winter precipitation receipt during El Niño is significantly different ($\alpha = .1$) from winter precipitation during La Niña only in regions one, five, and ten. Summer precipitation during El Niño is not significantly different from summer precipitation during La Niña in any region. These results illustrate the important point that while on average, El Niño precipitation receipt is significantly different from precipitation received during La Niña across Hawaii, individual events show a greater fluctuation in precipitation receipt within each region.

Table 4. Average Precipitation Receipt within Regions, Based on Mann-Whitney Test^a

	Winter precipitation La Niña vs. El Niño <i>p</i> -value	Summer precipitation La Niña vs. El Niño <i>p</i> -value
Region 1	<i>.030</i>	.432
Region 2	.432	.149
Region 3	.343	.755
Region 4	.268	.876
Region 5	<i>.018</i>	.530
Region 6	.202	.530
Region 7	.268	.639
Region 8	.149	.755
Region 9	.149	.755
Region 10	<i>.073</i>	.343

^aSignificant *p*-values italicized.

Finally, none of the Kruskal-Wallis tests show significant differences ($\alpha = .1$) in precipitation anomalies across individual regions during El Niño and La Niña in both the concurrent winter and the following summer. Therefore, during a particular phase of ENSO, average precipitation receipt in different regions of Hawaii during winter and summer has the same anomaly sign across the islands. While the principal components analysis showed that there are clearly regions in Hawaii with different seasonal precipitation patterns, the Kruskal-Wallis tests indicate that variability across regions does not appear to be caused by ENSO and are more likely the result of other processes.

Synoptic patterns. To identify the atmospheric processes leading to the above relationships, we examined the winter (November–April) synoptic circulation patterns associated with El Niño and La Niña. An examination of mean 1000 mb geopotential heights shows the changes in pressure in the north-central Pacific (Fig. 5), which in turn result in variation in subsidence and precipitation patterns in Hawaii. During El Niño events, the subtropical high pressure cell present in the eastern north Pacific expands to the west (Fig. 5A), resulting in increased subsidence and decreased precipitation across the islands as a whole. During La Niña events the anticyclone is concentrated in the eastern North Pacific (Fig. 5B), and subsidence is weakened over Hawaii allowing for increased rainfall. Regarding geopotential height anomalies, during El Niño events anomalously low pressure is found to the north of the islands at the 1000 mb level (Fig. 5C) while during La Niña, the reverse pattern is found (Fig. 5D). This relationship is also present at the 850 mb and 700 mb levels (not shown). For El Niño events, the 500 mb level is average or slightly below average over Hawaii with above average heights to the north, while during La Niña events, the 500 mb level is above average over Hawaii, with below average heights to the north (not shown). This analysis shows that ENSO affects circulation patterns over the North Pacific, which in turn affect precipitation receipt in Hawaii.

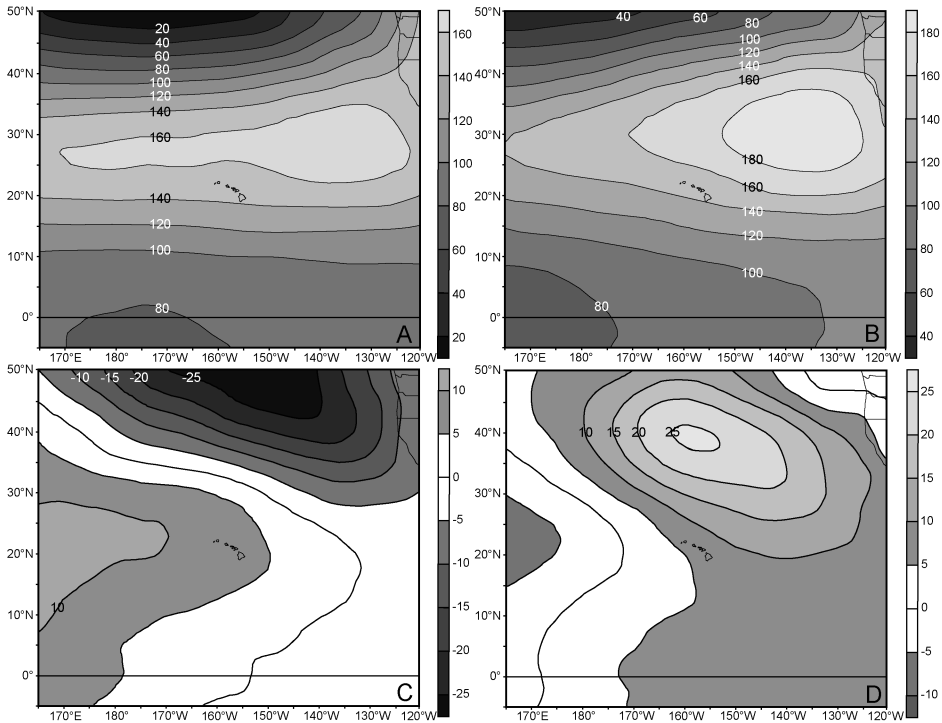


Fig. 5. Mean winter (Nov–Apr) 1000 mb heights (m) during El Niño (a) and La Niña (b). 1000 mb geopotential height anomalies (m) during El Niño (c) and La Niña (d). The subtropical high pressure cell expands to the west during El Niño and remains concentrated in the eastern north Pacific during La Niña. Regarding anomalies, the heights are below average to the north of Hawaii during El Niño and above average to the north of Hawaii during La Niña. *Source:* Image provided by the NOAA-CIRES Climate Diagnostics Center, Boulder, Colorado, from their Web site (<http://www.cdc.noaa.gov/>).

These circulation shifts are evident in the vector wind anomalies, which indicate that, during La Niña, windspeeds are slightly higher than during El Niño at the surface level (Fig. 6), consistent with typical behavior of stronger trade winds during La Niña. Surface winds are near average during El Niño and slightly above average during La Niña. Furthermore, trade wind directions are more easterly during La Niña, while during El Niño they have a slight northerly component. In an examination of dry winters and interactions between ENSO and the PDO, Chu and Chen (2005) found that weakened trade winds during El Niño/+PDO likely contribute to reduced rainfall across the islands.

The analysis of outgoing longwave radiation composites for El Niño and La Niña confirms the precipitation relationship found in this and other studies. During El Niño, larger OLR values are seen from 5°N to 30°N, indicating clearer skies with less convection and precipitation (Fig. 7). The opposite pattern is apparent for the La Niña composite. From 10°N to 25°N, below average OLR is recorded, indicating greater convection and precipitation over the islands.

In general, there is thus a set of synchronized circulation and precipitation changes for Hawaii associated with ENSO. While these are clear general

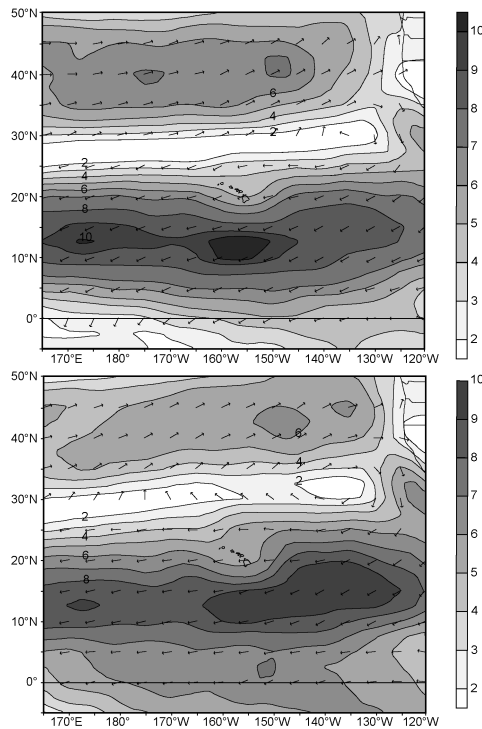


Fig. 6. Winter (Nov–Apr) surface windspeed anomalies during El Niño (top) and La Niña (bottom). Windspeeds are slightly slower during El Niño than during La Niña, and La Niña events are characterized by easterly winds while wind direction has a slight northerly component during El Niño events. *Source:* Image provided by the NOAA-CIRES Climate Diagnostics Center, Boulder, Colorado, from their Web site (<http://www.cdc.noaa.gov/>).

relationships at the synoptic scale, there are important local variations within the state that are highlighted in the regionalization analysis. While local climates are important in a location with the topographical variation of Hawaii, the Kruskal-Wallis test shows, however, that the ENSO-related circulation changes affect precipitation across the islands uniformly; during either phase of ENSO, seasonal precipitation variability responds consistently across all regions.

DISCUSSION AND CONCLUDING REMARKS

In this study, a principal components analysis was used to determine precipitation regions for the Hawaiian Islands based on the seasonality and variability of monthly precipitation rather than the overall quantity of precipitation used in a similar study (Lyons, 1982), and using roughly double the number of stations. The resulting regions are consistent with known seasonal precipitation patterns, and provided a way to examine the relationship between ENSO and precipitation at the sub-island level. Leeward and windward stations were divided into separate regions on all islands, and Maui, with a greater density of stations, was further divided by elevation.

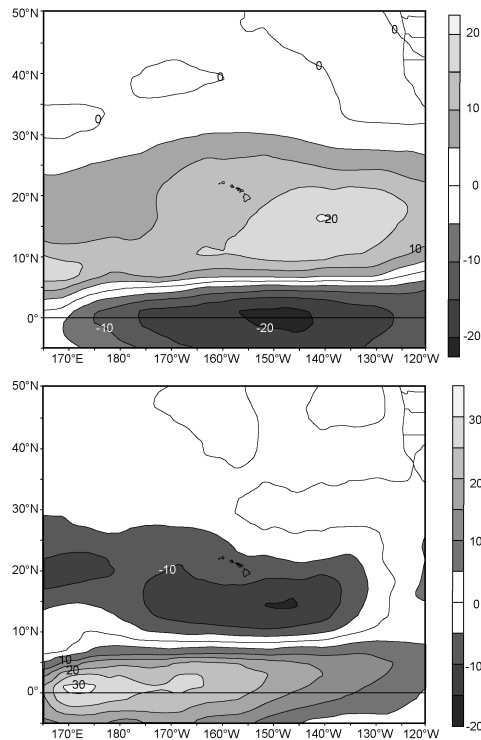


Fig. 7. Winter (Nov–Apr) outgoing longwave radiation (OLR) during El Niño (top) and La Niña (bottom). Above average OLR during El Niño indicates decreased convection and below average precipitation, while below average OLR during La Niña indicates enhanced convection and increased precipitation. *Source:* Image provided by the NOAA-CIRES Climate Diagnostics Center, Boulder, Colorado, from their Web site (<http://www.cdc.noaa.gov/>).

The regionalization presented here represents just one way in which the Hawaiian Islands can be partitioned based on the variability and seasonality of precipitation; other regional demarcations are possible depending on the nature and purpose of the analysis. The regionalization could be improved with the inclusion of more stations that have a long period of record, particularly a greater number of high-elevation stations. Molokai and northern Oahu have a sparse network of stations eligible for inclusion in this study, and Kauai and Hawaii lack a distribution of middle to high elevation stations. The confidence in the regionalization in those areas would be improved with a greater number of stations distributed over a broader area. Additionally, the statistical analyses could be improved through the use of a longer data record of precipitation that includes a greater number of El Niño and La Niña events, which would permit the use of more powerful (when underlying assumptions such as normality are met) parametric techniques (Pagano and Gauvreau, 2000).

Precipitation anomalies across regions differ between ENSO phases, and the spatial precipitation anomaly patterns of individual ENSO events can vary greatly.

For forecasting purposes, this confirms that while El Niño (La Niña) events generally result in lower (higher) precipitation, on average, any particular event can result in varied precipitation across the islands. Additionally, El Niño events more reliably result in below average precipitation as compared to La Niña events, which often but not always result in above average precipitation. Perhaps most importantly, our results explicitly illustrate that the effects of an individual El Niño or La Niña event are uniform across the islands; for a given phase of ENSO, the islands are wetter or drier everywhere as opposed to the increase or decrease in rainfall being concentrated in certain areas. It is with this finding in particular that our study contributes most significantly to the large body of literature on climate variability in Hawaii because while others have conducted a regional analysis of Hawaiian precipitation (Lyons, 1982), the relationship between ENSO and the seasonality of precipitation has not specifically been examined at the sub-island scale using statistical analyses.

At the sub-island scale the results of the correlation analyses between ENSO indices and precipitation in each region illustrate that the relationships are complex and that different areas of Hawaii have a different relationship with the various ENSO indices analyzed in this study. This observation has implications for seasonal precipitation forecasting. SOI and Niño 3.4 are more widely correlated with precipitation, and are perhaps more important in forecasting ENSO-related precipitation variability in Hawaii than Niño 1+2. The complexity of between-region relationships, in which some indices are positively associated with precipitation and others negatively correlated, suggests that future work should further examine the detailed atmospheric causes that result in these relationships. These might include mesoscale interactions of airflow and moisture transport with topography.

The synoptic circulation changes associated with ENSO are consistent with other studies and are generalizable to precipitation variability across the state. Combined with the results of the Kruskal-Wallis tests, the changes in pressure and subsidence patterns during El Niño and La Niña result in uniform changes in precipitation across the islands; there are not regional differences in rainfall receipt during a particular phase of ENSO.

Our future work with these regions concerns health applications linking climate variability and mosquitoes as disease vectors. The uniformity of the effects of El Niño and La Niña on precipitation will aid in the creation of a temporal and spatial model of mosquito habitat. In particular, given that precipitation varies uniformly across the islands during either ENSO event, mosquito habitat as explained with climate variability will likely fluctuate uniformly as well. Additionally, we feel the results presented here are potentially useful to water resources managers who may rely on the prediction of ENSO-related precipitation for management decisions, and could be applied in agricultural decision-making for predictive planting.

Acknowledgments: The authors thank Michael Crimmins for helpful comments and suggestions on the study, and Peter Johnson for technical assistance.

REFERENCES

- Barnston, A. G. and He, Y. (1996) Skill of canonical correlation analysis forecasts of 3-month mean surface climate in Hawaii and Alaska. *Journal of Climate*, Vol. 9, 2579–2605.
- Chu, P-S. and Clark, J. D. (1999) Decadal variations of tropical cyclone activity over the central North Pacific. *Bulletin of the American Meteorological Society*, Vol. 80, No. 9, 1875–1881.
- Chu, P-S. and He, Y. (1994) Long-range prediction of Hawaiian winter rainfall using canonical correlation analysis. *International Journal of Climatology*, Vol. 14, 659–669.
- Chu, P-S., Nash, A. J., and Porter, F-Y. (1993) Diagnostic studies of two contrasting rainfall episodes in Hawaii: Dry 1981 and Wet 1982. *Journal of Climate*, Vol. 6, 1457–1462.
- Chu, P-S. and Wang, J. (1997) Tropical cyclone occurrences in the vicinity of Hawaii: Are the differences between El Niño and non-El Niño years significant? *Journal of Climate*, Vol. 10, 2683–2689.
- Chu, P. S. (1989) Hawaiian drought and the Southern Oscillation. *International Journal of Climatology*, Vol. 9, 619–631.
- Chu, P. S. and Chen, H. (2005) Interannual and interdecadal rainfall variations in the Hawaiian Islands. *Journal of Climate*, Vol. 18, 4796–4813.
- Clark, J. D. and Chu, P-S. (2002) Interannual variation of tropical cyclone activity over the central north pacific. *Journal of the Meteorological Society of Japan*, Vol. 80, No. 3, 403–418.
- Climate Diagnostics Center. (2005) *Monthly/Seasonal Climate Composites*. NOAA-CIRES. Accessed November 2005 from <http://www.cdc.noaa.gov/cgi-bin/Composites/printpage.pl>
- Climate Prediction Center. (2005) *Frequently Asked Questions Regarding CPC's Current Monthly Atmospheric and SST Index Values*. Accessed February 15, 2007, from <http://www.cpc.ncep.noaa.gov/data/indices/Readme.index.shtml>
- Climate Prediction Center. (2006) *Cold and warm episodes by season*. Accessed June 2004 from the National Weather Service website, http://www.cpc.ncep.noaa.gov/products/analysis_monitoring/ensostuff/ensoyears.shtml
- Comrie, A. C. and Glenn, E. C. (1998) Principal components-based regionalization of precipitation regimes across the Southwest United States and Northern Mexico, with an application to monsoon precipitation variability. *Climate Research*, Vol. 10, 201–215.
- Dilley, M. and Heyman, B. N. (1995) ENSO and disaster: Droughts, floods, and El Niño/Southern Oscillation warm events. *Disasters*, Vol. 19, No. 3, 181–193.
- Giambelluca, T. W. and Nullet, D. (1991) Influence of the trade-wind inversion on the climate of a leeward mountain slope in Hawaii. *Climate Research*, Vol. 1, 207–216.
- Giambelluca, T. W., Nullet, M. A., Ridgley, M. A., Eyre, P. R., Moncur, J. E. T., and Price, S. (1991) *Drought in Hawaii, Report R88*. Honolulu, HI: Department of Land and Natural Resources.

- Giambelluca, T. W., Nullet, M. A., and Schroeder, T. A. (1986) *Rainfall Atlas of Hawai'i, Report R76*. Honolulu, HI: State of Hawaii, Department of Land and Natural Resources.
- Hales, S., Weinstein, P., Souares, Y., and Woodward, A. (1999) El Niño and the dynamics of vectorborne disease transmission. *Environmental Health Perspectives*, Vol. 107, No. 2, 99–102.
- Hanley, D. E., Bourassa, M. A., O'Brien, J. J., Smith, S. R., and Spade, E. R. (2003) A quantitative evaluation of ENSO indices. *Journal of Climate*, Vol. 16, 1249–1258.
- Juvik, J. O. and Nullet, D. (1994) A climate transect through tropical montane rain forest in Hawaii. *Journal of Applied Meteorology*, Vol. 33, 1304–1312.
- Kolivras, K. N. (2006) Mosquito habitat and dengue risk potential in Hawaii: A conceptual framework and GIS application. *Professional Geographer*, Vol. 58, No. 2, 139–154.
- Kovats, R. S. (2000) El Niño and human health. *Bulletin of the World Health Organization*, Vol. 78, No. 9, 1127–1135.
- Lyons, S. W. (1982) Empirical orthogonal function analysis of Hawaiian rainfall. *Journal of Applied Meteorology*, Vol. 21, 1713–1729.
- Nullet, D. and Giambelluca, T. W. (1992) Radiation climatology through the trade-wind inversion on the lee slope of Haleakala, Maui, Hawaii. *Physical Geography*, Vol. 13, No. 1, 66–80.
- Nullet, D., Juvik, J. O., and Wall, A. (1995) A Hawaiian mountain climate cross-section. *Climate Research*, Vol. 5, 131–137.
- Pagano, M. and Gauvreau, K. (2000) *Principles of Biostatistics, 2nd edition*. Pacific Grove, CA: Thomson Learning.
- Ramage, C. S. and Schroeder, T. A. (1999) Trade wind rainfall atop Mount Waialeale, Kauai. *Monthly Weather Review*, Vol. 127, 2217–2226.
- Riehl, H. (1949) Some aspects of Hawaiian rainfall. *Bulletin of the American Meteorological Society*, Vol. 30, No. 5, 176–187.
- Sanderson, M. (1993) *Prevailing Trade Winds*. Honolulu, HI: University of Hawaii Press.
- Sprent, P. (1993) *Applied Nonparametric Statistical Methods*. New York, NY: Chapman and Hall.
- Stidd, C. K. and Leopold, L. B. (1951) The geographic distribution of average monthly rainfall, Hawaii. *Meteorological Monographs*, Vol. 1, No. 3, 24–33.
- Swetnam, T. W. and Betancourt, J. L. (1992) *Temporal Patterns of El Niño/Southern Oscillation—Wildfire Patterns in the Southwestern United States*. Cambridge, UK: Cambridge University Press.
- Taylor, G. E. (1984) Hawaiian winter rainfall and its relation to the Southern Oscillation. *Monthly Weather Review*, Vol. 112, 1613–1619.
- Thiebaux, H. J. and Zwiers, F. W. (1984) The interpretation and estimation of effective sample size. *Journal of Climate and Applied Meteorology*, Vol. 23, 800–811.
- White, D., Richman, M., and Yarnal, B. (1991) Climate regionalization and rotation of principal components. *International Journal of Climatology*, Vol. 11, 1–25.